Hindawi
Advances in Materials Science and Engineering
Volume 2018, Article ID 8475384, 14 pages
https://doi.org/10.1155/2018/8475384

Research Article

Experimental and Simulation Study on Diffusion Behavior of Chloride Ion in Cracking Concrete and Reinforcement Corrosion

Yongchun Cheng, Yuwei Zhang, Chunli Wu, and Yubo Jiao

College of Transportation, Jilin University, Changchun, Jilin 130025, China

Correspondence should be addressed to Chunli Wu; clwu@jlu.edu.cn

Received 30 November 2017; Revised 28 March 2018; Accepted 12 April 2018; Published 25 June 2018

Academic Editor: Jun Liu

A chloride ion is a key factor affecting durability of reinforced concrete (RC) structures. In order to investigate chloride migration in cracked concrete, considering the mesoscopic heterogeneity of concrete, concrete modeled here is treated as a four-phase composite consisting aggregate, mortar, crack, and interfacial transition zone (ITZ). In this paper, two-dimensional finite element models of cracked concrete with different crack widths and crack quantity are established and the control parameters are determined based on the nonsteady-state chloride migration (NSSCM) test. In addition, based on the concrete finite element models, influences of crack width, crack quantity, and erosion time on chloride migration behaviors and characteristics are studied. Furthermore, a prediction model of chloride concentration on the simulated surface of a rebar in concrete influenced by different crack states is established. This model is used to derive the corrosion current density and corrosion depth prediction models of a rebar in this paper, which can be used by engineers to estimate the migration behaviors of chloride and rebar corrosion degree in RC structures in a short time and evaluate the duration of RC structures after knowing the status of cracks and chloride diffusion sources.

1. Introduction

Carbonation, freeze-thaw cycles, and chloride penetration of concrete are the important factors for reinforced concrete (RC) structures. Chloride ions penetrated into concrete cause rebar corrosion. As a corrosion process, rust appears on the surface of a rebar, which induces greater volume of the rebar and cracks of concrete cover [1]. Meanwhile, reinforced concrete will form cracks due to material shrinkage, thermal gradients, and repeated vehicle loading. Cracks lead to greater chloride migration power under the action of higher osmotic pressure, which leads a greater contact area between chloride ions and concrete and greater chloride concentration in concrete. In addition, more chloride ions migrate into concrete, more hydrated basic calcium chloride ($CaCl_2 \cdot Ca(OH)_2 \cdot H_2O$) will produce due to the reaction of chloride ions with calcium hydroxide ($Ca(OH)_2$). This reaction breaks the balance between hydrated calcium silicate (CSH) and $Ca(OH)_2$, which reduces adhesion stress between mortar and aggregate and leads to greater collapsibility on the surface of concrete. Therefore, chloride migration is harmful for concrete material properties and durability of RC structures. Hence, for durability prediction of RC structures, the consideration of influences of crack states on chloride migration in concrete is necessary.

The experimental researches and theoretical modeling about the influence of a crack on chloride migration in cracked concrete are abundant. Some researchers induced a crack on the surface of concrete by loading [2] and prefabricating metal sheet [3, 4] and then immersed concrete specimens into chloride solution for analyzing the influences of crack on chloride penetration coefficient [5] and chloride migration depth [6] of concrete. Djerbi et al. [7] examined the effects of traversing cracks of concrete on chloride diffusion and established an empirical model about the chloride diffusion coefficient in the crack zone. In addition, based on Fick's second law, Vol [8] and Gérard and

Marchand [9] as well as Yan et al. [10] established discrete, dispersive, and dual porous medium model of chloride diffusion in cracked concrete, respectively. The models were well used to describe the process of chloride penetration. However, these models ignored the mesoscopic heterogeneity of concrete material and merely regarded concrete as a one-dimensional and single-phase media material. Therefore, these models cannot fully describe the process of chloride migration at different zones in concrete. Moreover, for experimental studies, although they can provide much valuable data, it is still difficult to reveal the nonlinear process of chloride diffusion in concrete due to the different complexities of the experiments, different induced ways of cracks, and different precision of the experiment condition as well as the discrete experimental results. Nowadays, researchers tend to adopt the numerical technique to better analyze the mechanism of chloride penetration in cracked concrete as the fast progress of computer science. For example, Wang and Zhang [11] as well as Bentz et al. [12] developed two-dimension finite element models of cracked concrete to investigate the mechanism of chloride penetration in concrete. Wang and Ueda [13] as well as Liu et al. [14] proposed a two-dimension finite element migration model for understanding the process of chloride penetration in cracked concrete, in which the concrete was regarded as a three-phase composite, containing mortar, aggregates, and interfacial transition zones (ITZs). They found that the existence of cracks improved the ability of chloride penetration, and chloride ions can penetrate into the crack with a higher speed than they do into mortar and ITZs. However, all these finite element models treated the aggregates as circular areas, which is not consistent with real concrete cross section and ignores the special chloride diffusion path. So these models do not have a good practical value for the real concrete materials.

In this paper, a numerical study combined with the experimental results was presented to investigate the mechanism of chloride ions penetrating into cracked concrete more intuitively and theoretically. Two-dimensional finite element models of cracked concrete with different crack widths and crack quantity were established, and the control parameters were determined based on the nonsteady-state chloride migration (NSSCM) test. The chloride migration theory was determined by saturability equation amendatory Fick's second law and mass conservation equation. Based on the concrete finite element models, influences of saturability, crack width, crack quantity, and erosion time on chloride migration behavior and characteristics were studied. Moreover, a prediction model of chloride concentration at the location of the rebar in the concrete finite element model influenced by different crack states was established. Combined with Faraday's law, the chloride concentration prediction model was also used to derive the corrosion current density and corrosion depth prediction models of the rebar in this paper, which can be used by engineers to estimate the migration behavior of chloride and rebar corrosion degree in RC structures in a short time and evaluate duration of RC structures after knowing the states of cracks and chloride migration sources.

Table 1: Mixture proportions of the specimens.

Materials	Nominal proportions
Cement	433 kg/m^3
Water	195 kg/m^3
Fine aggregate	567 kg/m^3
Coarse aggregate	1205 kg/m^3
w/c	0.45

2. Chloride Migration Experiment

2.1. Mixture and Specimen Preparation. Based on the requirements of GB 175-2007 [15], PO 42.5 ordinary Portland cement is used in this study. Crushed stone (basalt in Jilin province) with diameters ranging from 2.36 mm to 20.00 mm and natural sand with a fineness modulus of 2.7 are required as coarse and fine aggregates, respectively. Specimens used in this study are composed of four concrete specimens and four mortar specimens with zero to three cracks, and there are three samples in each crack condition group for concrete specimens and mortar specimens. Mixture proportions of the concrete specimens used in this study are listed in Table 1. It should be noted that the mixture proportions of mortar specimens are the same with the concrete ones except the coarse aggregate. The slump result of this mixture is tested to be 40 mm, which means it is with favorable cohesiveness and meets well with the requirement of GB50164-2011 [16].

The artificial crack in the specimen by means of position required copper sheets with different quantity, and the distance between two cracks is set to 25 mm. The details of the single cracked specimen as an example are shown in Figure 1. Cylinders of $\phi 100\,\text{mm} \times 50\,\text{mm}$ are cast in plastic modules and compacted by a vibrating table. Copper sheets with 0.1 mm thickness are posited at the required position. The specimens are allowed to cure at the condition of 20°C and 95% relative humility (RH). The copper sheets are removed from the specimens after 4 h curing. The specimens are removed from moulds after 24 h curing. After that, all the specimens are cured under the normal curing condition (20°C and 95% RH) for 28 days before further experiments according to the China National Standard GB 175-2007.

2.2. Nonsteady-State Chloride Migration Test. According to GB/T 50082-2009 [17], vacuum saturated treatment must be performed before the chloride migration test. Firstly, put the specimens into stainless steel-based vacuum desiccators and decrease the vacuum pressure to 5 KPa in 5 min by a vacuum pump. Hold the 5 KPa vacuum pressure condition for 3 h. Subsequently, fill the desiccator with deionized water to immerse specimens, and maintain the vacuum pressure for one additional hour. Then, turnoff the vacuum pump to normalize vacuum pressure in desiccators. Finally, continuously immerse the specimens in desiccators by deionized water for 18 hours. After the vacuum saturated treatment, according to China National Standard GB/T 50082-2009 [17] and European Standard NT-BUILD492 [18], the cylindrical specimens are put in the test setup of NSSCM as

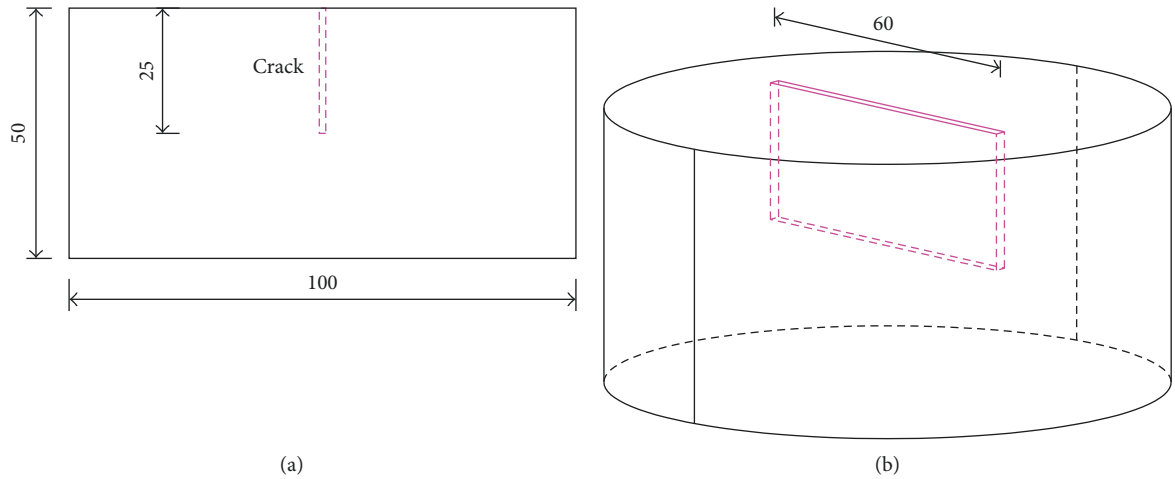

Figure 1: Specimen dimension (unit: mm). (a) Front view. (b) Stereoscopic view.

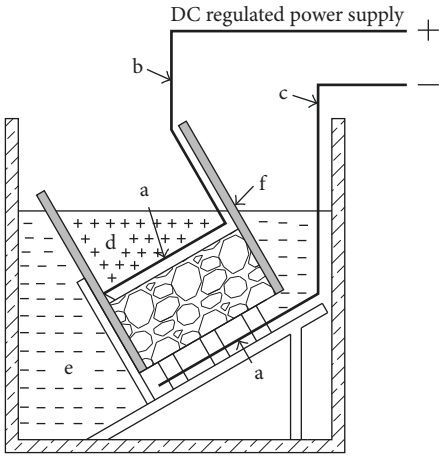

(a) Anode and cathode metal plate
(b) Anode
(c) Cathode
(d) Anolyte (NaOH solution)
(e) Catholyte (NaCl solution)
(f) Rubber drum

Figure 2: Experimental setup for the NSSCM test.

shown in Figure 2 for performing the chloride migration test at 20°C. In this test, the chloride ions can migrate in the direction of the vertical axis under the action of an external electric medium from surface to interior of concrete material quickly. After required time of the NSSCM test, the specimens are removed from the test setup and cut into half along the axis parallel to the direction of placement by loading. Spray the cutting plane with silver nitrate ($AgNO_3$) solution and then measure the acreage of visible white (silver chloride precipitation) area. Depth of chloride penetration X is calculated by the following equation:

$$X = \frac{A}{L} = \frac{\int_0^L dS}{L}, \tag{1}$$

where X is the depth of the chloride penetration, A is the measured acreage of the visible white area, and L is the length of the specimen bottom, 50 mm.

In this experiment, the chloride diffusion coefficient is given by the following equation:

$$D = \frac{0.0239\,(273+T)}{(U-2)t} \times \left[X - 0.0238\sqrt{\frac{HX\,(273+T)}{(U-2)}}\right], \tag{2}$$

where D is chloride diffusion coefficient (m^2/s), U is the absolute value of the external application voltage (V), T is the average of initial and final temperatures of the anode (°C), H is the thickness of the specimen (mm), X is the average depth of the chloride penetration (mm); and t is the time during the chloride penetration test (h).

2.3. Experimental Results and Discussion. Figures 3 and 4 show the chloride penetration area details in concrete specimens and mortar specimens.

It can be seen that depths of the chloride penetration in the concrete specimens are larger than the mortar specimens. The reason is that initial current of the mortar specimens is larger than that of the concrete specimens, so the applied external voltage for the mortar specimens should be less than that of the concrete specimens according to requirements of GB/T 50082-2009 and NT-BUILD492. Hence, concentration of the chloride ions migrated in the mortar specimens is larger than that in the concrete specimens. In addition, it can be observed that the chloride ions migrate into concrete not only along the parallel axis of cracks but also along the vertical axis of cracks, which can be concluded that the way of chloride migration in the crack zone of concrete is two-dimensional. Moreover, the chloride penetration depth for the crack is higher than the uncracked zone in concrete, and it is indicated that the chloride penetration coefficient of the cracked zone is higher than that of the uncracked zone in concrete.

In the NSSCM test, the chloride penetration depth values (X) of mortar specimens and concrete specimens are listed in Tables 2 and 3, respectively. The calculated chloride penetration coefficients of mortar specimens and concrete specimens are shown in Figure 5.

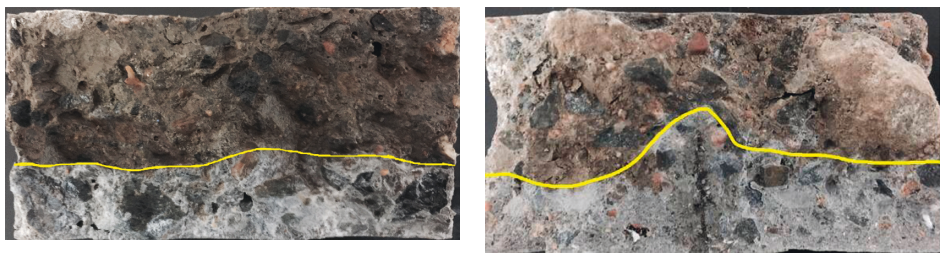

(a) (b)

Figure 3: Chloride penetration area in the concrete specimens. (a) Uncracked concrete specimen. (b) Concrete specimen with 1 crack.

(a) (b)

Figure 4: Chloride penetration area in the mortar specimens. (a) Uncracked mortar specimen. (b) Mortar specimen with 3 cracks.

Table 2: Chloride penetration depth (X) in the mortar specimens (mm).

Mortar specimens	#1 specimen	#2 specimen	#3 specimen	Average value	Standard deviation
Uncracked	10.31	10.65	10.56	10.50	0.17
1 crack	10.98	11.38	11.92	11.42	0.47
2 cracks	11.85	12.56	12.11	12.17	0.36
3 cracks	12.71	12.96	13.26	12.97	0.28

Voltage: 25 V; time: 24 h.

Table 3: Chloride penetrate depth (X) in the concrete specimens (mm).

Concrete specimens	#1 specimen	#2 specimen	#3 specimen	Average value	Standard deviation
Uncracked	16.86	16.12	17.45	16.81	0.67
1 crack	19.16	18.22	18.64	18.67	0.47
2 cracks	19.89	20.37	20.52	20.26	0.33
3 cracks	20.92	22.65	22.19	21.92	0.90

Voltage: 30 V; time: 24 h.

From Tables 2 and 3 and Figure 5, it can be concluded that the average of the chloride penetration depth and coefficient is improved along with the increase of crack quantity. The chloride penetration depth of the concrete specimens is a little higher than that of the mortar specimens, and the reason is that chloride ions penetration ability of ITZs (the zone between aggregate and mortar) is higher than that of mortar [7, 19].

The $AgNO_3$-based colorimetric method is the traditional way for measurement of chloride penetration in concrete. Although operation of this method is easy, it is limited by the minimum chloride concentration for coloring $AgNO_3$.

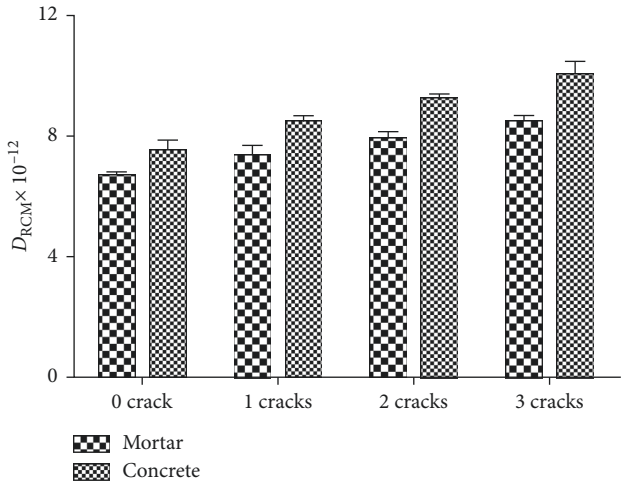

Figure 5: Chloride penetration coefficient for mortar and concrete materials (m^2/s).

Hence, this traditional method did not give a very clear boundary of chloride penetration, and it is difficult to reveal the influence of the crack on chloride migration in concrete exactly. Because of the fast advantage of computer science and computational mathematics, performing a numerical study can better illustrate this issue and deeply analyze the impacts of the crack on chloride migration.

3. Simulation Study on Chloride Migration in Cracked Concrete

3.1. Theoretical Background about Chloride Migration Model. In this study, concrete is considered as a semi-infinite medium, and there are no chemical bond and physical

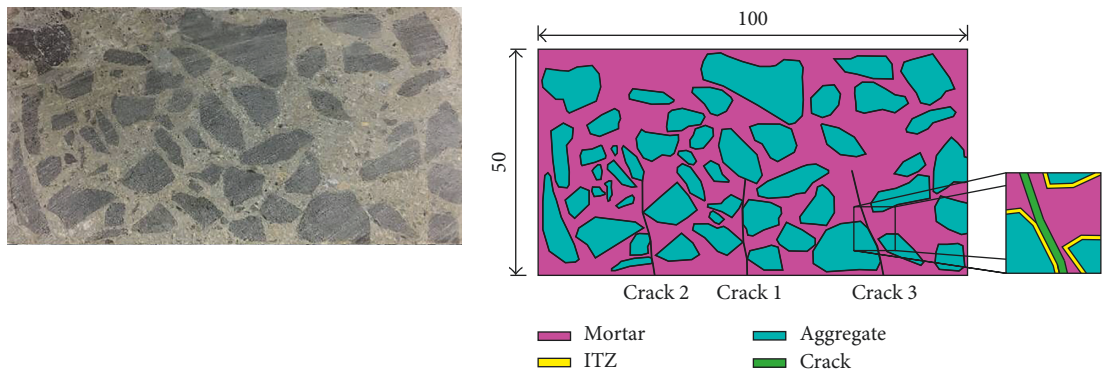

Figure 6: Concrete numerical model. (a) Concrete cross section. (b) Four-phase numerical model.

bond between chloride ions and anhydrous binders. For saturated concrete, chloride ions migrate into concrete by ionic diffusion because of the existence of concentration gradient between external solution and the pore solution of concrete material. The migration action of chloride ions in saturated concrete can be described by Fick's first law:

$$J_i = -\left[D_i \frac{\partial C_i}{\partial x} \vec{i} + D_i \frac{\partial C_i}{\partial y} \vec{j} \right], \tag{3}$$

where J_i is the flux of the chloride ions in phase i, D_i is the chloride diffusion coefficient in phase i, and C_i is the chloride concentration in phase i.

During the chloride migration process, the attenuation of chloride penetration ability can be determined as follows:

$$D_i = D_{i0} \left(\frac{t_0}{t} \right)^m, \tag{4}$$

where D_{i0} is the diffusion coefficient at the moment of t_0 (28 days), t is the time of chloride penetration, and m is the constant of attenuation of chloride penetration ability, 0.52 [20].

Moreover, migration of chloride can be expressed in terms of the mass conservation and current conservation, which is defined as Fick's second law:

$$\frac{\partial C_i}{\partial t} = -\nabla J_i. \tag{5}$$

Furthermore, concrete material is often unsaturated in majority of exposure environments for RC structures. For unsaturated concrete, the diffusion coefficient affected by relative humidity is determined as follows [21, 22]:

$$D_{i\theta} = D_i \left[1 + \left(\frac{1-\theta}{1-\theta_c} \right)^4 \right]^{-1}, \qquad \theta = \frac{\Theta - \Theta_i}{\Theta_s - \Theta_i}, \tag{6}$$

where $D_{i\theta}$ is the diffusion coefficient affected by relative humidity in phase i; D_i is the chloride diffusion coefficient of saturated concrete in phase i; θ is the relative humidity; θ_c is the critical relative humidity level at which the diffusion coefficient drops in half, and the value is 0.83; Θ is the humidity of concrete; Θ_s is the humidity of saturated concrete; and Θ_i is the humidity of concrete in the initial state. This function is important for describing the coupling between the water (moisture) migration and the chloride ions migration. Numerical examples will be shown later for detailed analysis.

3.2. Multiphase Migration Model for Concrete with Mesocrack. Concrete is a heterogeneous material, in which the internal mesostructure affects the chloride penetration ability [14]. In this paper, cracked concrete is treated as a heterogeneous composite material of four constituent parts, namely mortar, aggregates, ITZs, and cracks, and each one is treat as one phase. In order to establish a numerical model better fitted with the actual concrete material, the polished uncracked concrete specimen used in the NSSCM test is used to take the image for obtaining the cross section, which is shown in Figure 6(a). Taking advantage of the actual concrete cross section and image processing technology, a two-dimensional four-phase concrete numerical model with 3 mesocracks is established as shown in Figure 6(b), in which the red zones represent mortar, yellow zones represent ITZ, blue zones represent aggregate, and green zones represent crack. Since the aggregates have much higher resistance to ionic diffusion than the other phases, they are assumed to be impermeable. In other words, ionic migration happens only in mortars, ITZs, and cracks. Outside aggregates, aureole of ITZ shells wrapping the aggregate is seen. The real thickness of ITZs in ordinary concrete is said to be 30 μm–80 μm [23]. Therefore, the thickness of ITZ layers is set to 50 μm in the present model. By the way, the mesocracks located at the edge of concrete bottom are created based on the principle of mechanics of fracture. The mesocrack quantity set in this model is from 0 to 3. In addition, according to the National Standard JTG D62-2004 [24], the maximum allowed crack width of reinforced concrete is 200 μm, so the mesocrack widths set in this model are 50 μm, 100 μm, 150 μm, and 200 μm.

3.3. Migration Parameters and Boundary Conditions. For the four-phase cracked concrete numerical model herein, the chloride diffusion coefficient in aggregates is defined as D_A.

Since the aggregates are assumed to be impermeable, the value of D_A is $0\,m^2/s$. The ionic diffusivity in the mortar phase is defined as D_M, which is determined by the NSSCM test, which equals to $6.69\times10^{-12}\,m^2/s$. In addition, the ionic diffusivity in ITZ phases (defined as D_I) is suggested to be 1.3–16 times that of in the mortar phases (defined as D_M) [14, 25, 26]. In this paper, D_I is set to 8 times of D_M, which equals to $5.35\times10^{-11}\,m^2/s$. For the chloride diffusion coefficient (defined as D_C) in the crack, Djerbi et al. [7] considered the value of the chloride diffusion coefficient in the crack is much larger than the coefficient in mortar. D_C is only related to crack width, and it has no relationship with the type of binder. The relationship between crack width and ionic diffusivity described by Djerbi is as follows:

$$D_{C1} = \begin{cases} 2\times10^{-11}w - 4\times10^{-10}, & 30 \le w \le 80\,\mu m \\ 14\times10^{-10}, & w > 80\,\mu m, \end{cases} \quad (7)$$

where w is the crack width (μm).

Meanwhile, Sahmaran [19] performed an experimental study and found that the relationship between ionic diffusivity and crack width can be determined by the function as follows:

$$D_{C2} = \left(34.58 + 0.002w^2\right)\times10^{-11}. \quad (8)$$

In this study, the chloride diffusion coefficient (D_C) in the crack phase can be calculated by the average value between (7) and (8); that is, $D_C = (D_{C1} + D_{C2})/2$. Hence, the values of D_C for $50\,\mu m$, $100\,\mu m$, $150\,\mu m$, and $200\,\mu m$ mescocrack widths set in this numerical model are $4.98\times10^{-10}\,m^2/s$, $9.74\times10^{-10}\,m^2/s$, $10.97\times10^{-10}\,m^2/s$, and $12.73\times10^{-10}\,m^2/s$, respectively.

Furthermore, deicing salt is often used in winter on the surface of RC bridges in order to melt the snow and avoid traffic accidents. Components of deicing salt are mainly sodium chloride (NaCl) and calcium chloride ($CaCl_2$). Hence, chloride ions in melted snow solution will penetrate into concrete gradually. Vu and Stewart [27] illustrated that the statistical mean value of chloride-accumulated concentration on the surface of RC bridges under the action of deicing salt in the cold region is $3.5\,kg/m^3$, the coefficient of variation is 0.5, and the distribution is lognormal. Zhang et al. [28] measured the chloride concentration on the surface of the girder and pier stud of overpass in Beijing under the action of deicing salt. The statistical mean concentration value is equal to $3.0\,kg/m^3$. Hence, the concentration of the chloride ions on the surface of concrete is equals to $3.5\,kg/m^3$ ($59.83\,mol/m^3$). Besides, the initial and boundary conditions can be determined and listed in Table 4. Element mesh of the concrete two-dimension multiphase numerical model used in the present study is shown in Figure 7, which is divided into the triangle mesh with the maximum unit size of 2 mm and the smallest unit size of 0.0075 mm according to the finite element analysis software FEA.

Table 4: Initial and boundary conditions.

Concentration boundary conditions	$y = 0$ mm	$C = 59.83\,mol/m^3$
	$y = 50$ mm	$C = 0\,mol/m^3$
Flux boundary conditions	$x = 0$ mm	$J = 0\,mol/m^3$
	$x = 100$ mm	$J = 0\,mol/m^3$
Initial boundary conditions	$t = 0$	$C = 0\,mol/m^3$

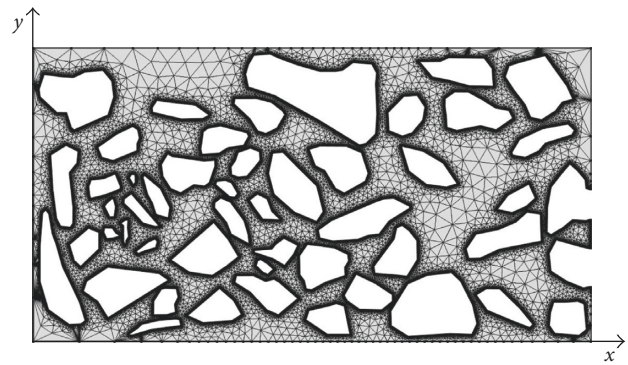

Figure 7: Element mesh of the concrete numerical model.

4. Simulation Results and the Prediction Model for Reinforcement Corrosion

4.1. Effect of Relative Humidity on Chloride Migration. In this section, based on the numerical model of the uncracked concrete and amendatory chloride migration equation (6), the effect of relative humidity in concrete on chloride migration is discussed. In general, moisture exists in pores of concrete in gaseous state and liquid state when the relative humidity in concrete is less than 45% and more than 45%, respectively [29]. Therefore, chloride migration concentration distribution profiles under 50%, 70%, and 100% relative humidity in concrete are simulated in this study, and the results are shown in Figure 8.

From Figure 8, it can be concluded that the depth of chloride migration in concrete reduces with the decrease of relative humidity. So, it is weak for the ability of chloride migration under a small value of relative humidity, which means that the action of chloride diffusion is restrained and chloride ions are gathered in some locations of concrete in this situation. When the relative humidity increases due to the existence of the new chloride solution on the surface of concrete, the previous gathered chloride ions combined with new chloride ions will increase the concentration gradient and ability of chloride diffusion. Hence, in cold regions, chloride ions solution made by melted snow and deicing salt will migrate into concrete and saturated concrete. Because of the evaporation of liquid solution, relative humidity in concrete reduces, diffusion of chloride ions is stopped, and they will gather in the superficial layer of the concrete cover. When the relative humidity is increasing again due to melting of snow by deicing salt, the new chloride ions combined with the previous gathered chloride ions will induce a more initial concentration of chloride diffusion, speed of chloride migration, total chloride flux, and depth of chloride migration. Therefore, it is serious for the durability of RC structures under the action of chloride solution wetting-drying cycles.

4.2. Effect of Crack Quantity on Chloride Migration. Crack quantity is a key parameter to estimate the damage degree of RC structures. Hence, the quantitative analysis of

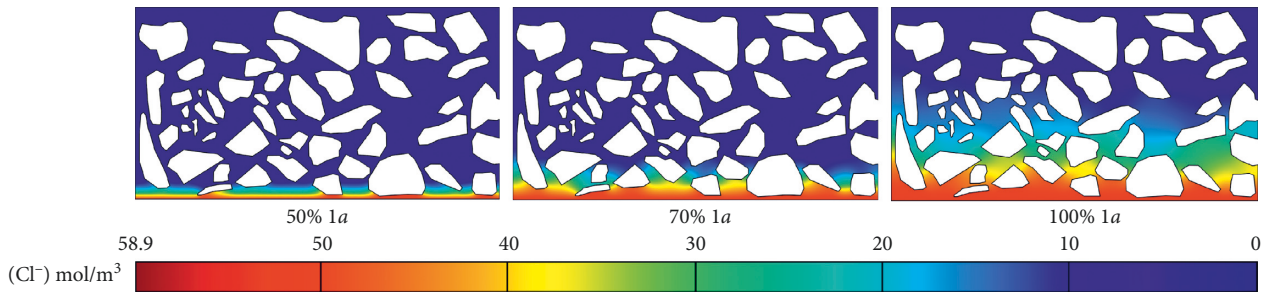

Figure 8: Concentration distribution profiles of the chloride ions under the effect of relative humidity in concrete at 1 year.

the effect of crack quantity on chloride diffusion is important for evaluating the durability of RC structures under chloride ions aggressive environment. In this section, the crack width is set to 0.20 mm and the quantity of cracks is set to 0–3 in the numerical models for analyzing the influence of crack quantity on chloride migration. Figure 9 shows the concentration distribution profiles of chloride ions in concrete with different crack quantities at different time within 1 year.

From Figure 9(a-i) and (b-i), it can be seen clearly from the profiles that when the crack exists in concrete, chloride concentration near the cracked zone increases rapidly and chloride concentration is higher in the cracked zone than that in other zones. From Figure 9(b), it can be observed that the chloride ions can migrate into concrete not only along with the parallel axis but also the vertical axis of cracks, which can be concluded that the way of chloride migration in the crack zone of concrete is two-dimensional. In addition, with the increase of crack quantity, the profile of the chloride ions migration increases and spreads to the whole concrete cross section gradually. All these phenomena are in a good agreement with the experimental study for chloride diffusion. Besides, from Figure 9(b-iii), (c-iii), and (d-iii), as a new crack occurs, the influence of the new crack on the chloride migration profile is significant at the crack zone but not significant at the zone away from the crack. From Figure 9(d), it can be concluded that the chlorine concentration in the middle of two adjacent cracks is greater than that of the chloride ions away from the crack, and the higher the crack quantity, the greater the penetration depth of the chloride ion in the same time. For the zones between two adjacent cracks, concentration of the chloride ions is lower than that at the tip of cracks. The greater crack quantity leads to a greater depth of chloride penetration.

Moreover, the average concentrations of the chloride ions penetration within 1 year in each whole simulated concrete model are calculated to better evaluate the effect of crack quantity on chloride flux (chloride concentration) in concrete. The results are shown in Figure 10.

As can be seen from Figure 10, with the increase of crack quantity, the average chloride ions concentration in the concrete is improved, which means that more chloride ions have penetrated into concrete. Moreover, the increase rate of chloride concentration per unit time is decreased with the increase of erosion time, which means that chloride concentrations have an attenuate tendency during the whole diffusion process.

4.3. Effect of Crack Width on Chloride Migration. For experimental studies, it is difficult for them to reveal effect of crack width on chloride migration in concrete because the self-healing of cracks leads to uncontrollable artificial crack widths [30, 31]. Also, qualities of specimens used in experiments are different, so the results of experimental studies are discrete and not compelling. To avoid the issues discussed above, numerical simulation is used to further analyze the effect of crack width on chloride migration in concrete in this section. Figure 11 shows the simulation results of the concentration distribution profiles of the chloride ions in concrete with different crack widths and crack quantities at 0.1 year.

As can be seen from Figure 11, it can be concluded that the areas of chloride migration (concentration distribution profile) are increasing with the increase of crack width and crack quantity. From Figure 11(a-i), (b-i), and (c-i), it can be seen that the concentration distribution profiles do not change much with the different quantity of 0.05 mm crack, which means that the effect of crack narrower than 0.05 mm on chlorine migration in concrete is not significant. Meanwhile, it can be seen from Figure 11(a-ii) and (b-ii), (a-iii) and (b-iii), and (a-iv) and (b-iv) that concentration distribution profiles of chloride ions are obviously enhanced, which means that a crack wider than 0.5 mm can significantly increase the concentration of chloride ions penetration into concrete. In addition, as can be seen obviously from Figure 11(b-iii) and (b-iv), concentration of the chloride ions at the tips of cracks and surrounding areas of cracks is increased with the increase of crack width, which shows that the increase of crack width leads to the expansion of chloride ions diffusion flux in concrete. Also, it can be inferred that the internal boundary of the crack will approximately equal to the concrete exposed boundary along with the increase of crack width. In this situation, chloride concentration internal of the crack is not determined by the process of chloride diffusion, and it directly equals to the concentration of chloride source on the surface of concrete. So a wide width of the crack can greatly accelerate the diffusion process of the chloride ions in concrete, and the influence of cracks on chloride ions diffusion will be more significant along with the increase of chloride ions erosion time.

At the same time, in order to further intuitively judge and quantify the impact of crack width on chloride migration in concrete, the average chloride concentration (diffusion flux) in the whole concrete cross section with different crack widths and crack quantities is calculated in

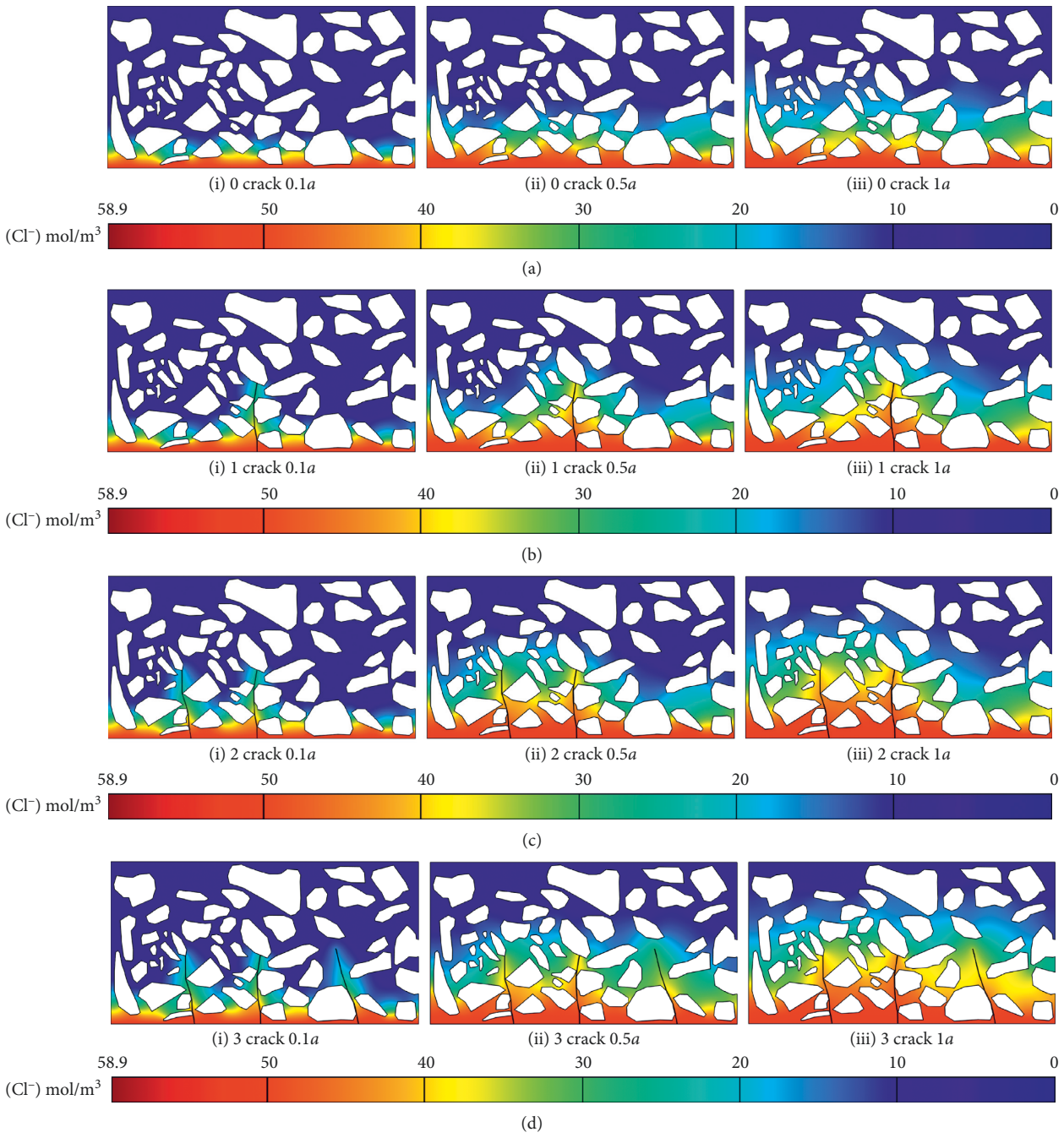

Figure 9: Concentration distribution profiles of chloride ions in concrete with different crack quantities within 1 year. (a) Uncracked concrete and concrete with (b) 1×0.2 mm crack, (c) 2×0.2 mm crack, and (d) 3×0.2 mm crack.

the numerical model within 1 year in different time, and the results are shown in Figure 12.

As can be seen from Figure 12, the average chloride diffusion flux is increased with the increase of crack width and crack quantity. Comparing with change of crack width from 0 mm to 0.05 mm, 0.10 mm to 0.15 mm, and 0.15 mm to 0.20 mm, the increment of the chloride ions diffusion flux is the most significant as the crack width increases from 0.05 mm to 0.10 mm. It shows that the chloride ions get more diffusion power for migrating into cracked concrete when the crack width reaches 0.05 mm and the acceleration process and influence scopes are obviously increased with the increase of the crack width.

4.4. Influence of Cracking on Reinforcement Corrosion. The rebar embedded in concrete is not prone to corrosion within a short time in sound concrete due to the high and stable alkalinity of concrete solution. From previous work in this study, cracks lead to a higher chloride diffusion coefficient of concrete under the action of the higher osmotic pressure in cracked concrete. Moreover, cracks of concrete cover often

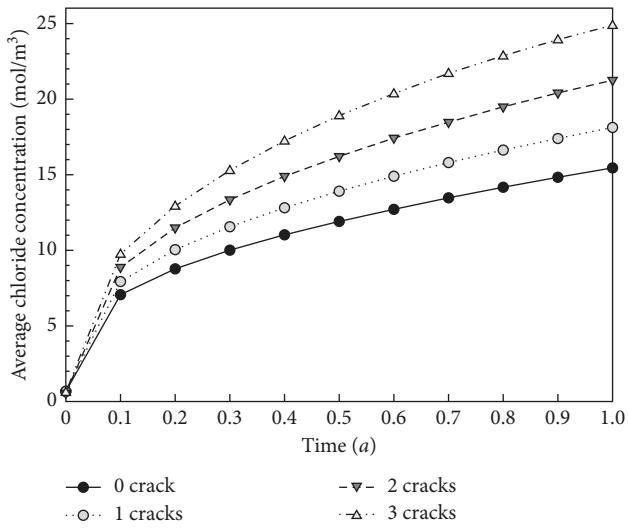

Figure 10: Average chloride concentration in concrete influenced by crack quantity.

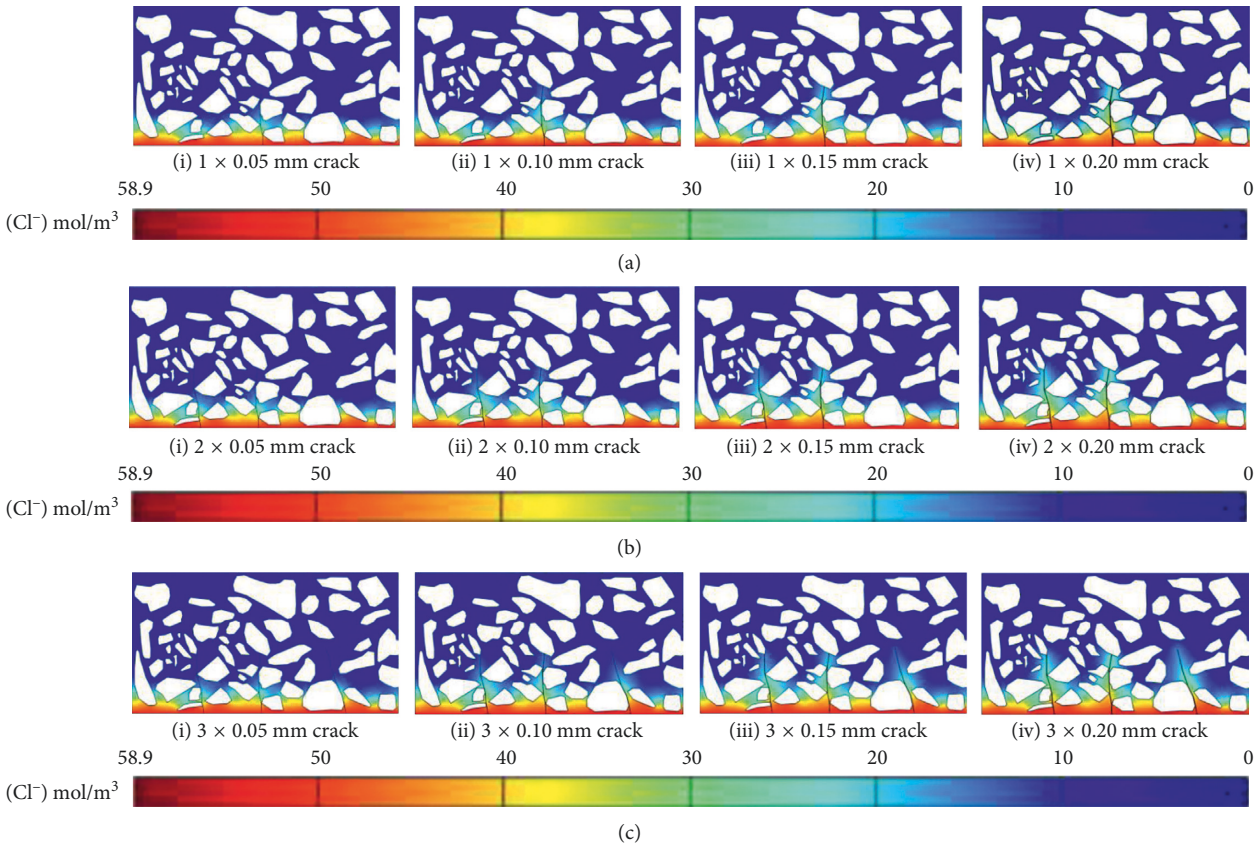

Figure 11: Concentration distribution profiles of chloride ions in concrete with (a) 1 crack, (b) 2 cracks, and (c) 3 cracks with different crack widths and crack quantities at 0.1 year.

provide a more easy access for ingress water and oxygen in concrete to the surface of the rebar, which results in accelerating corrosion of the rebar. Therefore, investigations on concentration of chloride ions on the surface of the rebar under the different crack and time conditions of chloride penetration are important to be pursued.

The depth of the concrete cover is the main factor affecting the steel corrosion; that is, the position of the rebar is affected by different concentrations of chloride ions. It should be noted that the depth of the concrete cover of 30 mm is used to interpret the influence of cracking on reinforcement corrosion in the numerical model of the

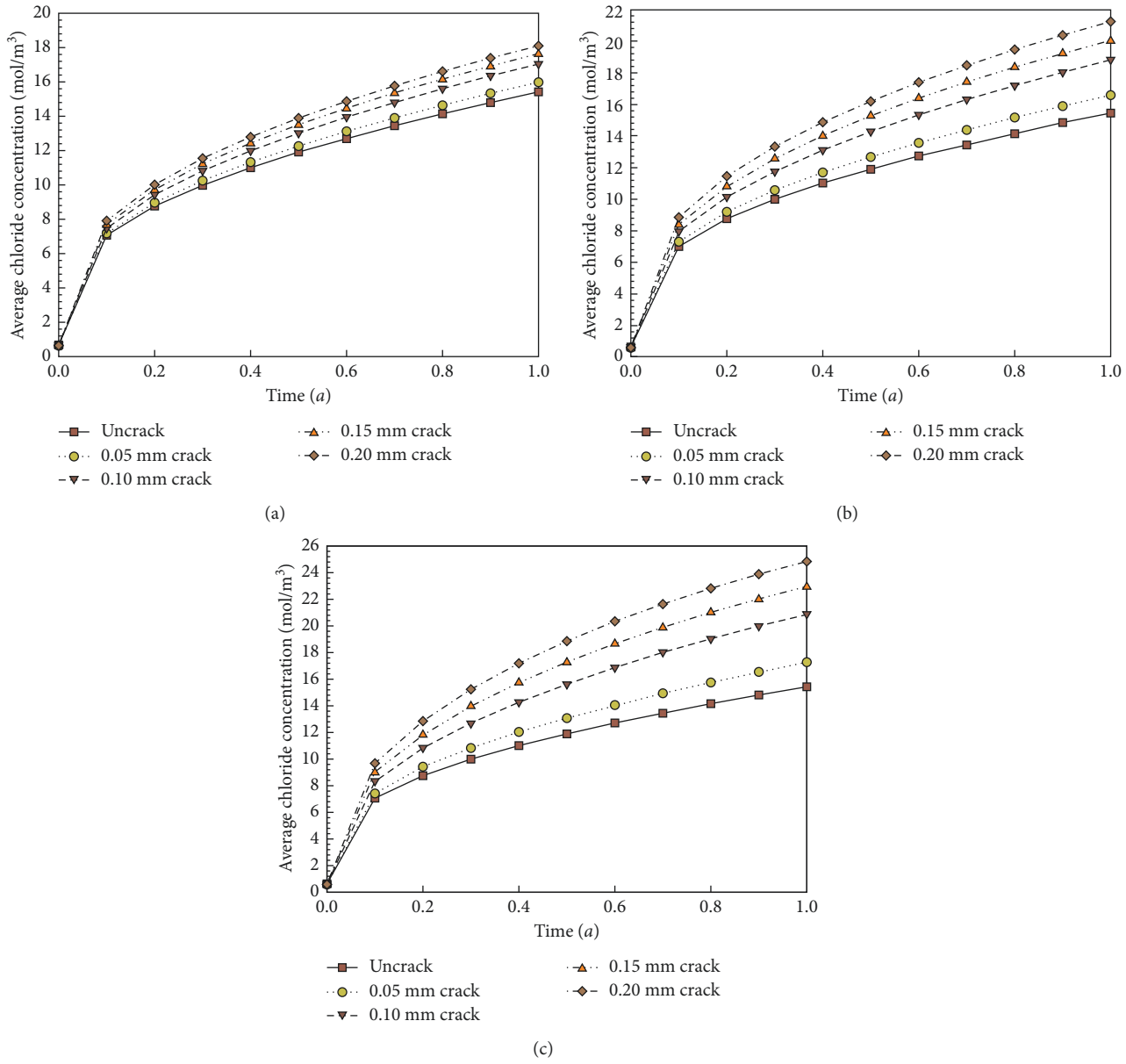

Figure 12: Comparisons of average chloride concentration on the surface of the rebar between models (different crack widths and quantities). Crack quantity: (a) 1, (b) 2, and (c) 3.

study. The concentrations of the chloride ions for the lines at the distance of 30 mm from the bottom edges of concrete models are calculated to establish the prediction model under different crack conditions. The other thicknesses of concrete cover can be studied by the proposed method, but they are not studied to save space.

For quantitatively analyzing this issue, concentration boundary ($y = 0$) is set to 1 (mol/m^3) and crack frequency is used to represent the quantity of cracks per meter. Hence, the values of crack frequency for 1, 2, and 3 cracks in concrete models used in this study are 10, 20, and 30 per meter in the models of this study. The location of the line for calculating the average chloride concentration in the

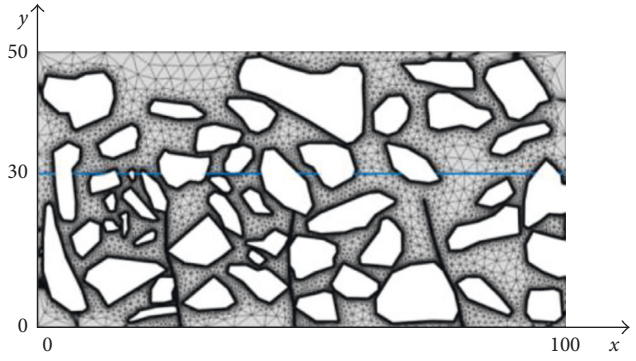

Figure 13: Calculation line for average chloride concentration.

Table 5: Values of the undetermined coefficients.

Coefficient	a	b	c	d	e	f	g	h	i	j
Value	5.01×10^{-2}	-8.41×10^{-2}	-3.28×10^{-3}	-4.18×10^{-1}	3.96×10^{-3}	1.91×10^{-2}	6.67×10^{-1}	8.03×10^{-2}	2.82×10^{-5}	5.35×10^{-2}

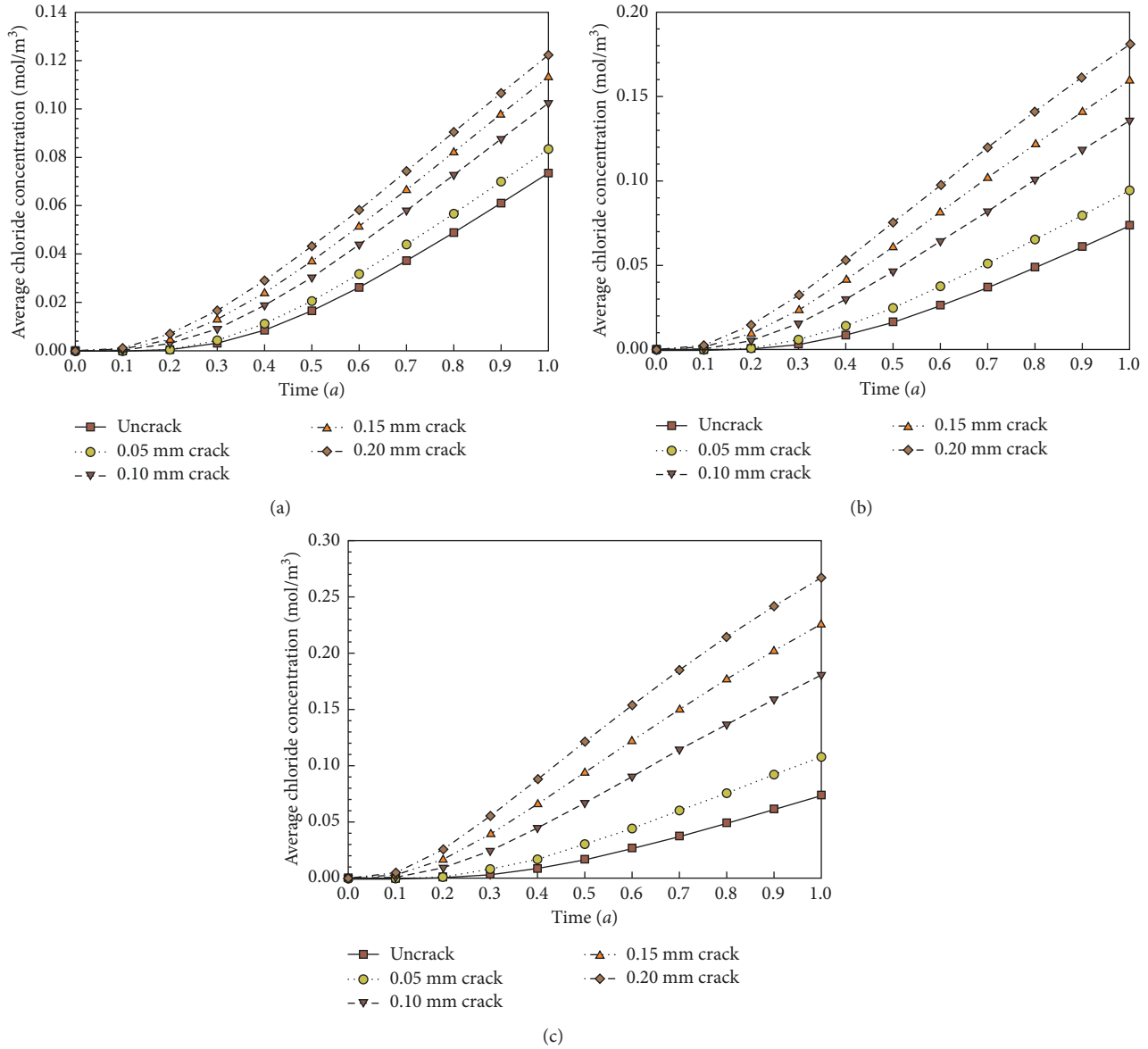

Figure 14: Comparisons of average chloride concentration on the surface of the rebar between models (different crack widths and frequency). . Crack frequency: (a) 10, (b) 20, and (c) 30.

numerical model is the blue one shown in Figure 13. The calculated results of average chloride concentrations on the simulated surface of the rebar under different conditions (erosion time, crack frequency, and crack width) are listed in Table 5. Based on Table 5, the curves of average chloride concentration on the simulated surface of the rebar related to different crack widths and frequencies are shown in Figure 14 to understand the tendency for the influences of cracks on rebar corrosion.

From Figure 14, it can be seen that the tendency of chloride concentration on the simulated surface of the rebar is increasing, which is as the same as that of chloride concentration in the whole concrete cross section. In addition, the increasing rate of chloride concentration on the simulated surface of the rebar is greater than that of chloride concentration in the whole concrete cross section along with the erosion time, and it can be indicated that the chloride ion can affect the corrosion behavior of the rebar in a short time. Moreover, from Figure 14, it can be concluded that, for the same crack width and crack frequency, chloride concentration increases linearly with the increase of erosion time. For the same erosion time and crack width, chloride concentration

Table 6: Statistical parameters.

R^2	F	P
0.974	646.994	4.16×10^{-118}

R^2 is the coefficient of association. The value approaching 1 represents a good correlation between data and regression equation. The larger the F value is, the more significant the regression equation is; P is the probability value of F value. The smaller the P value is, the more reliable the regression equation is. In summary, the regression equation is reliable for predicting concentration of chloride in concrete.

increases linearly with the increase of crack frequency. For the same crack frequency and erosion time, chloride concentration increases linearly with the increase of crack width. Therefore, considering the computational accuracy and convergence rate of the prediction model, a quadratic multivariate linear regression equation is established as the prediction model to quantitatively evaluate the concentration of chloride ions on the simulated surface of the rebar under the effect of erosion time, crack frequency, and crack width. The established regression equation is as follows:

$$C_{ST} = a + b \times T + c \times M + d \times D + e \times T \times M + f \times M \times D + g \times T \times D + h \times T^2 + i \times M^2 + j \times D^2, \quad (9)$$

where $a \sim j$ are undetermined coefficients of the regression equation, C_{ST} is the chloride concentration on the surface of the rebar embedded in concrete (mol/m^3), T is the time of chloride penetration (a), M is the crack frequency (quantity/m), and D is the crack width (mm). The least squares method is used for the regression analysis to fit the regression equation with simulated data, and the values of undetermined coefficients are listed in Table 5.

The statistical parameters of the regression equation is calculated and listed in Table 6.

Rebar corrosion is an electrochemical process. The corrosion current density (i_{corr}) of the rebar during the rebar corrosion process can be used to monitor the corrosion behavior such as corrosion rate. Qu [32] established an empirical model for i_{corr} of the rebar embedded in concrete related to climate and external environment by performing a controlled climate experiment for reinforced concrete. The model is as follows:

$$i_{corr} = 2.486\left(\frac{RH}{45}\right)^{1.6072}\left(\frac{T}{10}\right)^{0.3879}\left(\frac{w/c}{0.35}\right)^{0.4447} \cdot \left(\frac{d}{10}\right)^{-0.2761}(k)^{1.7376}, \quad (10)$$

where i_{corr} is the corrosion density (μA/cm^2), d is the depth of concrete cover (mm), w/c is the water cement ratio, and k is the content of chloride ions on the surface of rebar (%). RH is the relative humidity (%) and T is temperature (°C). Considering the control conditions of the models in this study and the most advantageous migration conditions for chloride ions, the value of RH, T, w/c, and d can be determined as 100%, 25°C, 0.45, and 30 mm, respectively. Hence, (10) can be rewrite as follows:

$$i_{corr} = 10.567 \times k^{1.7376}. \quad (11)$$

Base on (9) and (11), corrosion current density of the rebar under the effect of chloride migration is determined as follows:

$$i_{corr} = 10.567 \times \left(\frac{C_i \times C_{ST} \times M_{Cl^-}}{\rho_{Cl^-}}\right)^{1.7376}, \quad (12)$$

where C_{ST} is the chloride concentration on the surface of the rebar embedded in concrete (mol/m^3); C_i is the concentration of diffusion source on the surface of concrete (mol/m^3); M_{Cl^-} is the molar mass of the chloride ion, 35.5 g/mol; and ρ_{Cl^-} is the density of chloride solution (g/m^3). In general, it is believed that when the corrosion current density of the rebar reaches 0.1 (μA/cm^2), the rebar begins to rust.

Therefore, based on (9) and (11), corrosion behavior of the rebar embedded in concrete considered cracking situations, external environment conditions can be predicted, and corrosion time can be predicted by considering 0.1 μA/cm^2 as critical corrosion current density of rebar.

Besides, it is also suggested by researches that the durability of RC structures is seriously degraded when the corrosion depth of the rebar reaches more than 0.1 mm. Therefore, 0.1 mm can be treated as the critical corrosion depth of the rebar for predicting the service life of RC structures. The relationship between corrosion depth and corrosion current density of metal can be described by Faraday's law:

$$\delta_t = \frac{A i_{corr} t}{\rho_s n F}, \quad (13)$$

where δ_t is the corrosion depth of metal (mm); A is molar mass of iron ion, 56 g/mol; i_{corr} is the corrosion current density (μA/cm^2); t is the time of corrosion (a); n is the number of electrons of iron ion, $n = 2$; F is the Faraday constant, 9.65×10^4 C/mol; and ρ_s is the density of the rebar, 7.86 g/cm^2. Therefore, the prediction model for corrosion depth of the rebar can be established as follows by considering the nonuniformity of the corrosion current density under the conditions discussed in this study from time t_0 to t_1 based on (12) and (13):

$$\delta_t = 2.27 \times 10^{-9} \int_{t_0}^{t_1} (C_i \times C_{ST})^{1.7376} dt,$$

$$C_{ST} = 5.01 \times 10^{-2} - 8.41 \times 10^{-2} T - 3.28 \times 10^{-3} M - 4.18 \times 10^{-1} D + 3.96 \times 10^{-3} T \cdot M + 1.91 \times 10^{-2} M \cdot D + 6.67 \times 10^{-1} T \cdot D + 8.03 \times 10^{-2} T^2 + 2.82 \times 10^{-5} M^2 + 5.35 \times 10^{-2} D^2. \quad (14)$$

4. Conclusions

In this paper, based on the NSSCM test for concrete specimens, a numerical study is presented for investigating the mechanism of chloride ions in cracked concrete theoretically by establishing two-dimensional four-phase finite

element models of cracked concrete with different crack widths and crack quantities. Based on the concrete finite element models, influences of saturability, crack width, crack quantity, and erosion time on chloride migration behavior and characteristics are studied:

(i) The increase of crack quantity and crack width leads to a greater depth and diffusion flux of chloride penetration in concrete. That is, with the increase of crack width and crack quantity, chloride migration will aggravate.

(ii) The influence of relative humidity on the action of chloride diffusion is significant. Hence, chloride solution wetting-drying cycles will increase the concentration of chloride penetration sources in the superficial layer of the concrete cover, which is serious for the durability of RC structures.

(iii) Moreover, a regression equation for predicting chloride concentration is established based on the simulation results in this study, and two methods for predicting service life of RC structures are discussed in this study, which can be used by engineers to estimate the migration behavior of chloride and rebar corrosion degree in RC structures in a short time and evaluate duration of RC structures after knowing the status of cracks and chloride migration sources.

Conflicts of Interest

The authors declare that they have no conflicts of interest.

Acknowledgments

The authors express their appreciation for the financial supports of National Natural Science Foundation of China under Grant nos. 51478203 and 51408258.

References

[1] C. L. Page and K. W. J. Treadaway, "Aspects of the steel electrochemistry of steel in concrete," *Nature*, vol. 297, no. 5862, pp. 109–115, 1982.

[2] K. Wang, D. C. Jansen, S. P. Shah, and A. F. Karr, "Permeability study of cracked concrete," *Cement and Concrete Research*, vol. 27, no. 3, pp. 381–393, 1997.

[3] H. Ye, N. Jin, X. Jin, and C. Fu, "Model of chloride penetration into cracked concrete subject to drying–wetting cycles," *Construction and Building Materials*, vol. 36, no. 4, pp. 259–269, 2012.

[4] L. Marsavina, K. Audenaert, G. D. Schutter, N. Faur, and D. Marsavina, "Experimental and numerical determination of the chloride penetration in cracked concrete," *Construction and Building Materials*, vol. 23, no. 23, pp. 264–274, 2009.

[5] S. Mu, G. D. Schutter, and B. G. Ma, "Non-steady state chloride diffusion in concrete with different crack densities," *Materials and Structures*, vol. 46, no. 46, pp. 123–133, 2013.

[6] F. Q. He, *Measurement of Chloride Migration in Cement-based Materials Using $AgNO_3$ Colorimetric Method*, Ph.D. dissertation, Central South University, Changsha, China, 2010.

[7] A. Djerbi, S. Bonnet, A. Khelidj, and V. Baroghel-Bouny, "Influence of traversing crack on chloride diffusion into concrete," *Cement and Concrete Research*, vol. 38, no. 6, pp. 877–883, 2008.

[8] N. Vol, "Prediction of chloride ions ingress in uncracked and cracked concrete," *ACI Materials Journal*, vol. 100, no. 1, pp. 38–48, 2003.

[9] B. Gérard and J. Marchand, "Influence of cracking on the diffusion properties of cement-based materials: part I: influence of continuous cracks on the steady-state regime," *Cement and Concrete Research*, vol. 30, no. 1, pp. 37–43, 2000.

[10] Y. D. Yan, W. L. Jin, and H. L. Wang, "Chloride ingression in cracked concrete under saturated state," *Journal of Zhejiang University (Engineering Science)*, vol. 45, no. 12, pp. 2127–2133, 2011, in Chinese.

[11] X. Y. Wang and L. N. Zhang, "Simulation of chloride diffusion in cracked concrete with different crack patterns," *Advances in Materials Science and Engineering*, vol. 2016, Article ID 1075452, 11 pages, 2016.

[12] D. P. Bentz, E. J. Garboczi, Y. Lu, N. Martys, A. R. Sakulich, and W. J. Weiss, "Modeling of the influence of transverse cracking on chloride penetration into concrete," *Cement and Concrete Composites*, vol. 38, no. 2, pp. 65–74, 2013.

[13] L. Wang and T. Ueda, "Mesoscale modelling of the chloride diffusion in cracks and cracked concrete," *Journal of Advanced Concrete Technology*, vol. 9, no. 3, pp. 241–249, 2011.

[14] Q. F. Liu, J. Yang, J. Xia, D. Easterbrook, and L. Y. Li, "A numerical study on chloride migration in cracked concrete using multi-component ionic transport models," *Computational Materials Science*, vol. 2015, no. 99, pp. 396–416, 2015.

[15] GB175–2007, *Common Portland Cement*, National Standard of the People's Republic of China, Beijing, China, 2007, in Chinese.

[16] GB 50164-2011, *Standard for Quality Control of Concrete*, National Standard of the People's Republic of China, Beijing, China, 2011, in Chinese.

[17] GB/T 50082-2009, *Standard for Methods of Long-Term Performance and Durability of Ordinary Concrete*, National Standard of the People's Republic of China, Beijing, China, 2009, in Chinese.

[18] NT-BUILD492, *Nordtest method, Concrete, Mortar and Cement-Based Repair Materials: Chloride Migration Coefficient Form Non-Steady-State Migration Experiments*, Espoo, Finland, 1999.

[19] M. Sahmaran, "Effect of flexure induced transverse crack and self-healing on chloride diffusivity of reinforced mortar," *Journal of Materials Science*, vol. 42, no. 22, pp. 9131–9136, 2007.

[20] P. S. Mangat and M. C. Limbachiya, "Effect of initial curing on chloride diffusion in concrete repair materials," *Cement and Concrete Research*, vol. 29, no. 9, pp. 1475–1485, 1999.

[21] A. V. Saetta, R. V. Scotta, and R. V. Vitaliani, "Analysis of chloride diffusion into partially saturated concrete," *ACI Materials Journal*, vol. 90, no. 5, pp. 441–451, 1994.

[22] A. Ababneh, F. Benboudjema, and Y. Xi, "Chloride penetration in nonsaturated concrete," *Journal of Materials in Civil Engineering*, vol. 15, no. 2, pp. 183–191, 2003.

[23] X. L. Du, R. B. Zhang, and J. Liu, "Meso-scale numerical investigation on chloride diffusivity in cracked concrete," *Journal of Beijing University of Technology*, vol. 2015, no. 4, pp. 542–549, 2015.

[24] JTG D62-2004, *Code for Design of Highway Reinforced Concrete and Prestressed Concrete by Ultrasonic-Rebound*

Combined Method, National Standard of the People's Republic of China, Beijing, China, 2005, in Chinese.

[25] C. C. Yang, "Effect of the interfacial transition zone on the transport and the elastic properties of mortar," *Magazine of Concrete Research*, vol. 55, no. 4, pp. 305–312, 2003.

[26] J. Y. Jiang, G. W. Sun, and C. H. Wang, "Numerical calculation on the porosity distribution and diffusion coefficient of interfacial transition zone in cement-based composite materials," *Construction and Building Materials*, vol. 2013, no. 39, pp. 134–138, 2013.

[27] K. A. T. Vu and M. G. Stewart, "Structural reliability of concrete bridges including improved chloride-induced corrosion models," *Building Technique Development*, vol. 22, no. 4, pp. 313–333, 2000.

[28] K. Zhang, W. Q. Bao, and N. W. Liu, "The effect of ice salt on durability of bridges," in *Annual Meeting of the China Society of Civil Engineering*, Beijing, China, 2000, in Chinese.

[29] M. Krus and L. K. Kie, "Determination of the moisture storage characteristics of porous capillary active materials," *Materials and Structures*, vol. 31, no. 8, pp. 522–529, 1998.

[30] W. Khaliq and M. B. Ehsan, "Crack healing in concrete using various bio influenced self-healing techniques," *Construction and Building Materials*, vol. 2, pp. 349–357, 2016.

[31] N. Zakari Muhammad, A. Shafaghat, A. Keyvanfar et al., "Tests and methods of evaluating the self-healing efficiency of concrete: a review," *Construction and Building Materials*, vol. 112, pp. 1123–1132, 2016.

[32] F. Qu, *Durability Study and Service Life Prediction of Concrete Specimens under Salt Frozen Environment*, Ph.D. dissertation, Xi'an University of Science and Technology, Xi'an, China, 2014, in Chinese.